New Phytologist

Research

F-box protein CFK1 interacts with and degrades *de novo* DNA methyltransferase in Arabidopsis

Jiani Chen[1], Jie Liu[1], Jianjun Jiang[2,3], Shuiming Qian[1], Jingwen Song[4], Rachel Kabara[2], Isabel Delo[2], Giovanna Serino[5], Fengquan Liu[3], Zhihua Hua[4] and Xuehua Zhong[1,2]

[1]Wisconsin Institute for Discovery, University of Wisconsin-Madison, Madison, WI 53715, USA; [2]Laboratory of Genetics, University of Wisconsin-Madison, Madison, WI 53706, USA; [3]Institute of Plant Protection, Jiangsu Key Laboratory for Food Quality and Safety-State Key Laboratory Cultivation Base of Ministry of Science and Technology, Jiangsu Academy of Agricultural Sciences, Nanjing, Jiangsu 210014, China; [4]Department of Environmental and Plant Biology & Interdisciplinary Program in Molecular and Cellular Biology, Ohio University, Athens, OH 45701, USA; [5]Department of Biology and Biotechnology, Sapienza Università di Roma, Rome 00185, Italy

Author for correspondence:
Xuehua Zhong
Email: xuehua.zhong@wisc.edu

Received: *20 July 2020*
Accepted: *16 November 2020*

New Phytologist (2021) **229:** 3303–3317
doi: 10.1111/nph.17103

Key words: *Arabidopsis thaliana*, DNA methylation, epigenetics, F-box protein, post-translational modification, ubiquitin proteasome pathway.

Summary

- DNA methylation plays crucial roles in cellular development and stress responses through gene regulation and genome stability control. Precise regulation of DOMAINS REARRANGED METHYLTRANSFERASE 2 (DRM2), the *de novo* Arabidopsis DNA methyltransferase, is crucial to maintain DNA methylation homeostasis to ensure genome integrity. Compared with the extensive studies on DRM2 targeting mechanisms, little information is known regarding the quality control of DRM2 itself.
- Here, we conducted yeast two-hybrid screen assay and identified an E3 ligase, COP9 INTERACTING F-BOX KELCH 1 (CFK1), as a novel DRM2-interacting partner and targets DRM2 for degradation via the ubiquitin-26S proteasome pathway in *Arabidopsis thaliana*. We also performed whole genome bisulfite sequencing (BS-seq) to determine the biological significance of CFK1-mediated DRM2 degradation.
- Loss-of-function *CFK1* leads to increased DRM2 protein abundance and overexpression of CFK1 showed reduced DRM2 protein levels. Consistently, CFK1 overexpression induces genome-wide CHH hypomethylation and transcriptional de-repression at specific DRM2 target loci.
- This study uncovered a distinct mechanism regulating *de novo* DNA methyltransferase by CFK1 to control DNA methylation level.

Introduction

DNA methylation is a conserved epigenetic mark that plays critical roles in gene regulation and genome integrity by silencing transposons or repetitive sequences (Weber & Schubeler, 2007). Aberrant DNA methylation patterns, which can be a consequence of environmental stresses, are implicated in many diseases, including tumorigenesis and neurological disorders (Thompson & Robertson, 2017; Jin & Liu, 2018). Given that plants cannot escape from adverse environments, a precise regulation of DNA methylation is extremely important for proper growth and development under unfavourable conditions (Pikaard & Mittelsten, 2014).

In animals, DNA methylation occurs mostly in symmetric CG contexts across the genome that is established by the *de novo* methyltransferases DNMT3 and maintained by DNMT1 through DNA replication (Bird, 2002). In plants, DNA methylation at cytosines can occur in both symmetrical and asymmetrical sequence contexts: CG, CHG, and CHH (H = A, T, C) (Weber & Schubeler, 2007; Law & Jacobsen, 2010). Domains Rearranged Methyltransferase 2 (DRM2), an orthologue of mammalian DNMT3, is responsible for *de novo* DNA methylation in Arabidopsis (Cao & Jacobsen, 2002). The maintenance of CG methylation involves Methyltransferase 1 (MET1), orthologue of mammalian DNMT1. CHH and CHG methylation is maintained by three enzymes: DRM2, plant-specific Chromomethylase 2 (CMT2) and Chromomethylase 3 (CMT3) (Matzke & Mosher, 2014; Zhong, 2016; Wendte & Schmitz, 2018; Zhang *et al.*, 2018).

Targeting of DRM2 to specific genomic regions is achieved through RNA-directed DNA methylation (RdDM) (Matzke *et al.*, 2015; Zhong, 2016; Zhang *et al.*, 2018). The very first phase of the RdDM pathway involves the generation of 24-nucleotide (nt) short interfering RNAs (siRNAs), which is a prerequisite for the targeting of DRM2 to homologous genomic sequences (Deng *et al.*, 2016). Single-stranded RNA transcripts, generated by RNA polymerase IV, are replicated by RNA-directed RNA polymerase 2 to produce double-strand RNAs, which are then cleaved by Dicer-like 3 into 24-nt siRNAs and loaded into an Argonaute 4 (AGO4) protein complex

(Zilberman *et al.*, 2003; Xie *et al.*, 2004; Mosher *et al.*, 2008; Law & Jacobsen, 2010). The siRNA–AGO4 complex can bind to scaffold transcripts produced by RNA polymerase V (Pol V), and then recruit DRM2 to specific target loci through complementary base paring between 24-nt siRNAs and nascent Pol V transcripts (Zhong *et al.*, 2014). DRM3 is a catalytically inactive DNA methyltransferase homologous to DRM2 and plays a role in RdDM through a physical interaction with Pol V (Henderson IR, 2010; Zhong *et al.*, 2015). Recently, DRM2 was identified to interact with DEAD box RNA helicases U2AF56 Associated Protein 56 (UAP56a/b), which has the ability to associate with chromatin in reproductive tissues and may be crucial for plant development (Azevedo *et al.*, 2019). Understanding the regulation of DNA methyltransferase is fundamental for proper establishment of DNA methylation patterns to regulate biological processes.

Over the years, emerging evidence has indicated that DNA methyltransferases in both mammals and plants are co-ordinately controlled through several levels of regulation, including post-translational modifications (PTMs) and post-transcriptional regulation by microRNAs (miRNAs) (Denis *et al.*, 2011). Some miRNAs play vital roles in the control of DNA methyltransferases. For instance, overexpression of miR-29 family members in acute myeloid leukemia cells led to the downregulation of DNMT3a and DNMT3b at both transcript and protein levels, resulting in a reduction in global DNA methylation (Garzon R, 2009). The *DRM2* gene was also reported to be regulated by miRNA (i.e. miR-773a) (Jha & Shankar, 2014). Studies have shown that PTMs such as phosphorylation, sumoylation and ubiquitination play an indispensable role in regulating DNA methyltransferases. Ubiquitination is a widespread PTM that is associated with protein degradation involving three enzyme families: E1 (the activating enzyme), E2 (the conjugating enzyme), and E3 (ubiquitin ligases). E3 ubiquitin ligases recruit the substrate and mediate the transfer of ubiquitin to a lysine residue of the substrate. In many cases, polyubiquitylated substrates are recognised by the 26S proteasome for degradation (Vierstra, 2003; Marshall & Vierstra, 2019). Ubiquitination of DNMT1, triggered by acetylation through the acetyltransferase Tip60, is catalysed by E3 ligase UHRF1 and then recruited to proteasomes for degradation (Du *et al.*, 2010). Conversely, DNMT1 is stabilised by HDAC1 and the deubiquitinase Herpes Virus-Associated Ubiquitin-Specific Protease (Du *et al.*, 2010). In addition, DNMT1 phosphorylation affects its protein stability, enzymatic activity, and ability to interact with other proteins including UHRF1 (Bostick *et al.*, 2007; Hervouet *et al.*, 2010; Esteve *et al.*, 2011; Lavoie & St-Pierre, 2011). SUMOylation (small ubiquitin-like modifier attachment) of DNMT3a dampens its ability to interact with HDACs, whereas proteins involved in acetylation-triggered ubiquitination and deubiquitination regulate DNMT1 stability (Du *et al.*, 2010; Augustine & Vierstra, 2018). Similarly, Casein Kinase 2 (CK2)-mediate phosphorylation of DNMT3a represses its *de novo* DNA methyltransferase activity, and is required for the localisation of DNMT3a to heterochromatin (Deplus *et al.*, 2014). Mutations or genetic alterations of DNMTs are associated with various diseases, including cancer, neurological diseases and immunological diseases (Okano *et al.*, 1999; Robertson & Wolffe, 2000; Baets *et al.*, 2015; Norvil *et al.*, 2019).

In plants, very few studies have been conducted on PTMs of DNA methyltransferases. CMT3 is reported to be ubiquitinated by the ubiquitin E3 ligase JMJ24 for proteasomal degradation, which leads to reduced CHG methylation at specific endogenous loci and compromised H3K9me2 levels (Du *et al.*, 2015; Deng *et al.*, 2016). The DRM2 protein consists of N-terminal ubiquitin-associated (UBA) domains and a C-terminal methyltransferase (MTase) domain. Crystal structural analysis has revealed that the dimerisation through the MTase domain is crucial for DRM2 catalytic activity (Zhong *et al.*, 2014). The UBA domains are also required for DRM2 function in DNA methylation at specific loci or at a genome-wide level (Henderson IR, 2010; Zhong *et al.*, 2014). The UBA domains of Arabidopsis DRM2 bind Lys63-linked tetraubiquitin (Lys63-Ub_4) and Lys48-Ub_4, a signal for proteolysis (Raasi *et al.*, 2005), thus providing a potential connection of ubiquitin proteasome pathway with DRM2-mediated DNA methylation.

Recent studies have suggested a pivotal role of ubiquitination in DNA methylation. E3 ubiquitin ligase UHRF1-dependent ubiquitination of H3 at lysine 23 is critical for the recruitment of DNMT1 to DNA replication sites and the maintenance of DNA methylation in *Xenopus* extracts (Nishiyama *et al.*, 2013). Ubiquitination of H3 at lysine 18 by UHRF1 was also identified to be essential in DNMT1-mediated maintenance DNA methylation in mammalian cells (Qin *et al.*, 2015). In fission yeast, ubiquitin ligase component Cul4-based ubiquitination is involved in heterochromatin formation by forming a complex with Rik1, and the Clr4 histone methyltransferase (Jia *et al.*, 2005). Cul4 and DDB1, a homologous protein of Rik1, was reported to regulate DNA methylation through the recruitment of the histone methyltransferase DIM-5 protein to methylate H3 at lysine 9 in *Neurospora* (Zhao *et al.*, 2010). In Arabidopsis, H2B monoubiquitination at lysine 143 is implicated in controlling DNA methylation and gene silencing (Sridhar *et al.*, 2007). Despite these studies, the connection between ubiquitination and DRM2 function as well as the general regulation of DRM2 at the post-translational level remain largely unknown.

Here, we identified an F-box protein, termed COP9 SIGNALOSOME INTERACTING F-BOX KELCH 1 (CFK1), as a direct interacting partner of DRM2. CFK1 functions as a substrate receptor of the SKP1-CUL1-F-box^{CFK1} (SCF^{CFK1}) ubiquitin E3 ligase complex. Consistent with the model of SCF^{CFK1}-mediated DRM2 ubiquitination and degradation, we found that CFK1 affects the DNA methylation status at DRM2 target loci by bisulfite sequencing. Our findings reveal a molecular mechanism of DRM2 abundance control through the SCF^{CFK1} proteasome degradation pathway.

Materials and Methods

Plant materials, growth conditions and chemical treatments

All *Arabidopsis thaliana* used here were on the Columbia (Col-0) ecotype background. The T-DNA insertion mutant *cfk1*

(WiscDsLox506C02) was obtained from the Arabidopsis Biological Resource Center. The *drm1 drm2* mutants were from Steven Jacobsen's laboratory (Chan *et al.*, 2006; Henderson & Jacobsen, 2008). The seeds were surface sterilised with 70% ethanol plus 0.01% Triton X-100, washed twice with 100% ethanol, and then sprinkled onto plates containing half-strength Murashige and Skoog (½MS) medium with 0.8% agar. The seeds on ½MS plates were stratified in the dark at 4°C for 3 d before placing in the growth room under continuous light at 100 μmol m^{-2} s^{-1} at 22°C. The 10-d-old seedlings were then transferred into soil and grown under a set of fluorescence lamps (Philips; 40W) at 100 μmol m^{-2} s^{-1} and 16 h : 8 h, light : dark cycles at 23°C for desired developmental stages or for the chemical treatment as follows.

For MG132 treatment, the seedlings were transferred to liquid ½MS medium with either dimethyl sulfoxide (DMSO) (control) or 50 μM MG-132 (Sigma; M7449), and incubated for 16 h under continuous light with gentle shaking. For cycloheximide (CHX) treatment, the seedlings were transferred to liquid ½MS medium with 500 μM CHX (Dot Scientific Inc., DSC81040-1) for the indicated time followed by the immunoblot analysis.

For estradiol induction, a 25 mM 17-β-estradiol (Sigma; E8875) stock solution was prepared in DMSO. The seeds were directly germinated and grown on ½MS medium plates supplemented with 2 μM inducer β-estradiol for 7 d before collecting samples for immunoblot analysis.

Construction of plasmids and generation of transgenic plants

To generate CFK1 overexpression plants, the coding sequences of CFK1 were amplified from Arabidopsis cDNA, digested with *Bam*HI/*Sal*I, and ligated into a *Bam*HI/*Sal*I-digested pCAMBIA1306 vector. For the inducible promoter, the coding sequences of CFK1 fused with HA at the C-terminal were PCR-amplified, digested with restriction enzymes *Xho*I/*Spe*I, and ligated into a *Xho*I/*Spe*I digested β-estradiol-inducible XVE pER8 vector (Zuo, 2000). Primers are listed in Supporting Information Table S1. To generate constructs of pDRM2::gDRM2-FLAG and pDRM2::gDRM2-HA in protoplasts, DRM2 was amplified from Arabidopsis gDNA, digested with *Eco*RI/*Sal*I and ligated into *Eco*RI/*Sal*I-digested pPZP212 (Chen *et al.*, 2017) and HA-tagged pCAMBIA1300 vectors, respectively. All constructs were transformed into *Agrobacterium tumefaciens* (Strain GV3101) and the recombinant strains were then transformed into *cfk1* mutant or Col-0 by the floral dip method (Clough & Bent, 1998). T1 transgenic lines were screened in the medium supplemented with kanamycin followed by T2 screening with single copy insertion of 3 : 1 survival ratio in the medium supplemented with kanamycin. Homozygous T3 lines of pDRM2::gDRM2-FLAG in Col-0 or *cfk1* were used for the experiment.

For the yeast two-hybrid screen, the coding sequences of *CFK1*, *ASK1* and *ASK2* were directly amplified from Arabidopsis cDNA. The *CFK1* cDNA fragments were digested and ligated into the *Bam*HI/*Not*I sites in pGBK-T7 vector (Clontech). Both *ASK1* and *ASK2* coding sequences were digested and cloned into the *Eco*RI/*Bam*HI sites in pGAD-T7 vector (Clontech). The coding sequence of *DRM2* was amplified from cDNA and digested by *Eco*RI/*Bam*HI, and then fused in-frame to the 3′-end of the activation domain on pGAD-T7 (Clontech).

For split luciferase complementation assay, DRM2 and CFK1 were amplified from Arabidopsis cDNA, digested with *Bam*HI/*Sal*I. DRM2 and CFK1 cDNAs were ligated into *Bam*HI/*Sal*I-digested pCAMBIA1300-nLUC and pCAMBIA1300-cLUC, respectively. For bimolecular fluorescence complementation (BiFC), *Bam*HI/*Sal*I-digested pXY104 and pXY106, respectively. *Bam*HI/*Sal*I-digested FLAG-tagged pCAMBIA1306 and HA-tagged pCAMBIA1300 for co-immunoprecipitation.

Yeast two-hybrid screen

To test protein–protein interactions in yeast, the bait and prey vectors were separately transformed into two haploid yeast strains, AH109 and Y187 (Clontech), respectively, and then mated in pairs to generate diploid yeast cells that co-expressed both bait and prey proteins examined. The positive interactions were verified by growing the mated diploid yeast cells on a quadruple synthetic dropout media lacking Ade, His, Leu, and Trp and supplemented with 5-bromo-4-chloro-3-indolyl-α-D-galactopyranoside (X-α-Gal, 40 mg l^{-1}).

BiFC assay

CFK1 or ASK1 was cloned and fused with N-terminus of yellow fluorescent protein (YFP) (YFPN), and DRM2 was fused with the C-terminus of YFP (YFPC). DRM2-YFPC and YFPN-CFK1 or YFPN-ASK1 were then transformed into the *Agrobacterium tumefaciens* strain GV3101. *Agrobacterium* cultures were grown at 30°C overnight in lysogeny broth (LB) containing antibiotics (50 μM spectinomycin), resuspended in infiltration medium (100 mM $MgCl_2$, 10 mM MES, pH 5.6, 200 mM acetosyringone) to an OD_{600} 0.1, and infiltrated into the lower epidermis of young *N. benthamiana* leaves using a needleless syringe. After 36–48 h, the YFP signal was analysed by a Nikon A1R confocal microscope.

Split luciferase complementation assay

The split luciferase complementation assay was performed as described previously (Yang *et al.*, 2018). CFK1 and DRM2 were cloned and fused with cLUC and nLUC, respectively. *Agrobacterium tumefaciens* transformed with CFK1-cLUC and DRM2-nLUC were grown in LB at 30°C overnight and resuspended in infiltration medium (same as above) to OD_{600} 0.1. The bacterial suspensions were infiltrated into the lower epidermis of young *N. benthamiana* leaves for 36–48 h. Luciferin (Promega; P1041) was used as the substrate for firefly luciferase activity analysis. The luciferase activity was measured using chemiluminescence by ImageQuant™ LAS 4000.

Protoplast transfection

Protoplasts were isolated from 3- to 4-wk-old Arabidopsis plants (Col-0 and *cfk1*) according to the Yoo *et al.* protocol (Yoo *et al.*,

2007). In brief, leaves were prepared, immersed into the enzyme solution (0.4 M mannitol, 20 mM KCl, 20 mM MES pH 5.7, 1.5% w/v cellulose R10 (Yakult Pharmaceutical Industry Co. Ltd), 0.4% w/v macerozyme R10 (Yakult Pharmaceutical Industry Co. Ltd), 10 mM $CaCl_2$, 5 mM β-mercaptoethanol, and 0.1-% BSA), and incubated at room temperature in the dark with gentle shaking for 2 h. After digestion, protoplasts were filtered through 75-μM nylon mesh and washed twice with W5 solution (2 mM MES pH 5.7, 154 mM NaCl, 125 mM $CaCl_2$, and 5 mM KCl), then resuspended in W5 solution and recovered on ice for 40 min. The protoplasts were suspended in MMg solution (4 mM MES pH5.7, 0.4 M mannitol, and 15 mM $MgCl_2$). About 10^6 protoplasts were transfected with 10 μg of the indicated constructs (DRM2-HA, GFP empty vector) using 40% PEG solution (40% v/v PEG 4000 (Sigma; 81240), 0.2 M mannitol, and 100 mM $CaCl_2$), then resuspended in W5 solution and incubated overnight under the dark at room temperature, followed by immunoblot analysis.

Immunoprecipitation and co-immunoprecipitation assay

Immunoprecipitation experiment was performed as described previously (Chen *et al.*, 2016; Chen *et al.*, 2018). In brief, for DRM2 ubiquitination, 0.5 g of pDRM2::gDRM2-FLAG seedlings was ground into powder and homogenised in 2 ml IP buffer (50 mM Tris-HCl, pH 8, 150 mM NaCl, 5 mM $MgCl_2$, 5% glycerol, 0.1% Nonidet P-40, 1 mM DTT, 1 mM PMSF, and protease inhibitor cocktail tablet (Roche; 14696200)). The supernatant was incubated with 5 μl α-FLAG M2 magnetic beads and rotated at 4°C for 2.5 h. The bead-bound complex was washed four times with IP buffer at 4°C for 5 min each. Bound protein was released from beads by boiling in 2X SDS sample loading buffer and analysed by immunoblotting with α-FLAG and α-ubiquitin antibodies.

Co-IP was performed as previously described (Guo *et al.*, 2018). In brief, CFK1-HA with either DRM2-FLAG or empty FLAG vector were co-infiltrated into 3-wk-old *N. benthamiana* leaves. Samples were collected two d after infiltration. Half a gram of each sample was ground into powder and total protein was extracted by Co-IP buffer (10 mM HEPEs pH7.5, 100 mM NaCl, 1 mM EDTA, 10% glycerol, 0.5% NP-40, 1 mM PMSF and one pellet of the protease inhibitor/10 ml (Roche; 14696200)). The supernatant was incubated with 5 μl FLAG magnetic beads with constant rotation at 4°C for 2h. The beads were collected and washed once with Co-IP buffer without NP-40. Bound proteins were released from beads by boiling in 40 μl 2X SDS sample loading buffer and analysed by immunoblotting with α-FLAG and α-HA antibodies. Same protocol was used for Co-IP in transgenic Arabidopsis seedlings pDRM2::gDRM2-FLAG XVE::CFK1-HA. The supernatant was incubated with 4 μl HA tag monoclonal antibody (Invitrogen; 26183) with constant rotation at 4°C for 2h, followed by addition of 40 μl Dynabeads Protein G (Invitrogen; 10003D) with constant rotation at 4°C for 2.5 h. The following procedure was the same as above.

Immunoblots

Total protein was extracted with 5% SDS, separated on a 10% SDS-PAGE gel, and transferred to a nitrocellulose membrane. The membrane was blocked with 3% milk and incubated with horseradish peroxidase-conjugated anti-FLAG (Sigma; A8592) or anti-HA (Roche; 12013819001) or anti-Beta-ACTIN (Proteintech; 60008-1-lg). Immunoblots were developed using Clarity Western ECL substrate (Clarity Western Peroxide Reagent and Clarity Western Luminol/Enhancer Reagent) from Bio-Rad for digital imaging.

RNA extraction and quantitative RT-PCR

Samples were collected from 10-d-old seedlings or flowers grown under continuous light at 22°C. Total RNA was extracted using a PureLink™ RNA mini Kit (Invitrogen; 12183025); 1 μg RNA was treated with DNase I (New England Biolabs, NEB; M0303) and reverse transcribed into cDNA using First Strand cDNA Synthesis (NEB; M0368). Quantitative PCR was performed using the CFX96 Real-Time System (Bio-Rad) and Vazyme 2× ChamQ reagent for three technical replicates of each sample. The transcript level was calculated relative to ACTIN-7.

Chop-PCR

Genomic DNA was extracted from Col-0, *dd*, DRM2-FLAG/*dd* and *cfk1* plants from 100 mg ground plant tissue; 400 μl extraction buffer (0.35 M sorbitol, 100 mM Tris-HCl, 5 mM EDTA) was added into the powder, followed by 400 μl lysis buffer (200 mM Tris-HCl, 50 mM EDTA, 2 M NaCl, 2% CTAB) and 27 μl 10% Sarkosyl. Samples were incubated at 65°C for 30 min. Next, 650 μl chloroform : isoamyl alcohol (24 : 1) mixture was added and then centrifuged for 10 min at 4°C. The upper phase was transferred and 0.7 volume isopropanol was added before centrifuging for 10 min at 4°C. The pellet was washed with 500 μl 70% ethanol and centrifuged for 5 min to collect DNA.

In total, 5 μg genomic DNA was mixed with 10× NEB buffer to 38 μl volume, and then divided into two equal 19 μl aliquots; 1 μl *Hae*III or McrBC enzyme (NEB, 10 units μl^{-1}) was added to one aliquot, and 1 μl H_2O was added to the second aliquot as mock treatment. Both aliquots were incubated at 37°C for 1 h, and then heat inactivated at 65°C for 20 min; 2 μl of each sample was used for PCR reaction. The primers for *Hae*III and McrBC digestion are listed in Table S1.

Phylogenetic analysis

The homologues of *Arabidopsis thaliana* CFK1 in 16 green plants were annotated using Closing Target Trimming (Hua & Early, 2019) and grouped by OrthoMCL (Li, 2003). Protein sequences were aligned using MUSCLE (Edgar, 2004) and subjected to maximum likelihood method-based phylogenetic analysis using RAxML (Stamatakis, 2014). The resulting Newick tree was displayed and rooted to Smpeg0014 in FIGTREE (http://tree.bio.ed.ac.uk/).

Whole genome bisulfite sequencing and analysis

In total, 1 μg DNA was used for the generation of bisulfite sequencing library as previously described (Pignatta *et al.*, 2015). In brief, genomic DNA was isolated from flower tissue using DNeasy Plant Mini Kit (Qiagen; 69104) and 1 μg DNA was sheared to 300–400 bp using a Covaris S220 SonoLab 7.5. The sheared DNA was used to prepare a library using the Illumina TruSeq DNA PCR-Free Low Throughput Library Prep Kit (Illumina; 20015962). Bisulfite treatment was followed using the EZ DNA Methylation-Lightening Kit (Zymo Research; D5031) and the library was enriched by 10 cycles PCR amplification using the Kapa HiFi HotStart Uracil ReadyMix (Kapa Biosystems; KK 2801). The library was validated using the chloroplast gene and Sanger sequencing to ensure the conversion of cytosine (C) to thymine (T). The library was sequenced on an Illumina HiSeq 4000 system with 50 bp single end reads.

The raw sequence reads were trimmed using Trimmomatic-0.39 (Bolger *et al.*, 2014) and then mapped to the Arabidopsis TAIR10 reference genome with BSMAP-2.90 (Xi & Li, 2009). Samtools-1.9 was used to filter the mapping results to keep uniquely mapped reads (Li *et al.*, 2009). The numbers of methylated and unmethylated reads of cytosines were called using methratio.py in BSMAP-2.90 and only cytosines with coverage ≥ 5 were used for further analysis. For differentially methylated region (DMR) calling, both Methylkit-1.12.0 and Fisher's exact test were used (Li *et al.*, 2009). Only windows significant in both methods were kept. BEDTOOLS v.2.29.0 (Quinlan, 2014) and DEEPTOOLS v.3.3.1 (Ramirez *et al.*, 2014) were used to generate data for metaplot.

Results

DRM2 protein is degraded through the 26S proteasome pathway

Arabidopsis DRM2 possesses a rearranged C-terminal methyltransferase domain and N-terminal three tandem UBA domains. UBA domains are evolutionarily conserved from yeast to humans and normally associate with poly-ubiquitin chains, signals recognised by the 26S proteasome for protein degradation (Myung *et al.*, 2001; Zhong *et al.*, 2014). DRM2 UBA domains were shown to bind to poly-ubiquitin chains with a preference for Lys63-linked chains *in vitro* (Raasi *et al.*, 2005). To determine whether DRM2 is degraded by the 26S proteasome, we treated the Arabidopsis seedlings expressing FLAG-tagged DRM2 driven by its native promoter in *drm1 drm2* (pDRM2::gDRM2-FLAG/*dd*) with MG132, a membrane-permeable proteasome inhibitor known to block the degradation of ubiquitin-labeled proteins (Nolan *et al.*, 2017). We noted a slightly increased DRM2 protein level upon MG132 treatment relative to the mock treatment (Fig. 1a), suggesting that DRM2 protein is degraded through the 26S proteasome pathway.

As a further confirmation, we treated the Arabidopsis seedlings pDRM2::gDRM2-FLAG/*dd* with MG132. DRM2-FLAG proteins were immunoprecipitated using FLAG beads and examined for ubiquitination using anti-ubiquitin antibodies. An increased amount of poly-ubiquitinated DRM2 was observed after MG132 treatment, as evidenced by the high molecular mass forms of DRM2 (Fig. 1b). Together, these results suggested that the degradation of DRM2 protein is likely to be dependent on the ubiquitin-26S proteasome pathway.

CFK1 interacts with DRM2 *in vitro* and *in vivo*

Our prior DRM2 affinity purification and mass spectrometry identified several interesting proteins involved in the ubiquitination pathway (Zhong *et al.*, 2014). This includes an E2 ubiquitin conjugating enzyme, a subunit of a RUB-activating enzyme

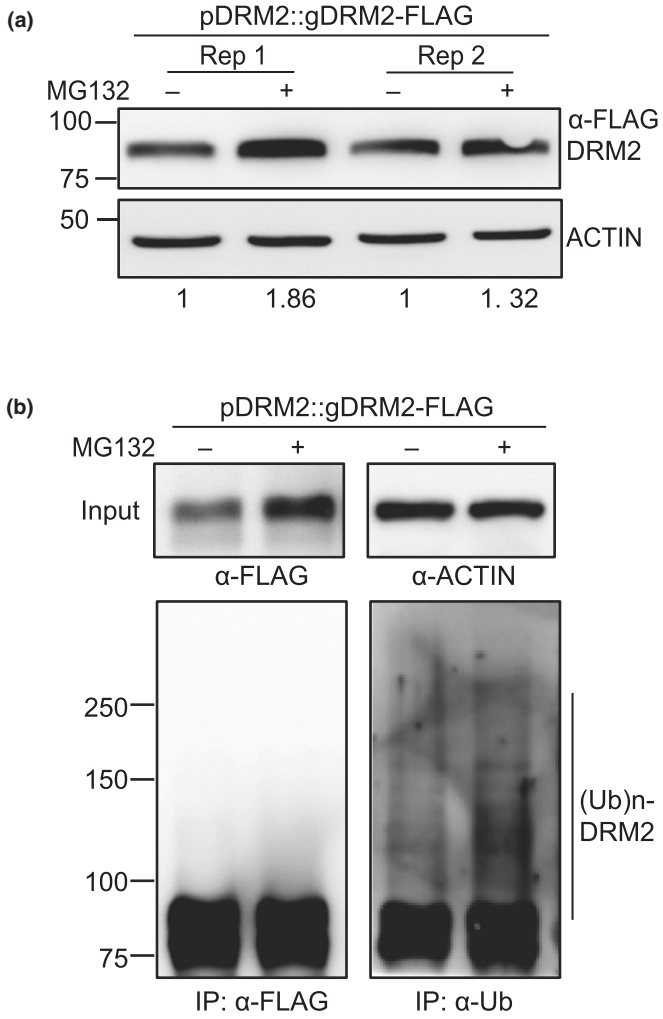

Fig. 1 DOMAINS REARRANGED METHYLTRANSFERASE 2 (DRM2) is degraded through the 26S proteasome pathway in Arabidopsis. (a) Immunoblot analysis showing the DRM2 protein level in *drm1 drm2* (*dd*) Arabidopsis seedlings expressing FLAG-tagged DRM2 under the control of its native promoter (pDRM2::gDRM2-FLAG) with or without MG132 treatment from two biological replicates (Rep 1 and Rep 2). ACTIN was used as a control. Numbers indicate the relative band intensity ratio of DRM2-FLAG to ACTIN, quantified by IMAGEJ software. (b) Immunoblot analysis showing the input (top) and immunoprecipitated DRM2 (bottom) in pDRM2::gDRM2-FLAG/*dd* transgenic Arabidopsis plants treated with or without MG132. ACTIN was used as a loading control.

analogous to the E1 ubiquitin-activating enzyme (ECR1), and a ubiquitin family protein (Table S2), indicating that DRM2 is likely to be targeted by an SCF ubiquitin E3 ligase. To identify the potential E3 ligase for DRM2, we searched through a group of conserved F-box proteins identified previously (Hua *et al.*, 2011; Hua *et al.*, 2013) and then directly tested their pairwise interactions with DRM2 using yeast two-hybrid screen assay. We discovered COP9 SIGNALOSOME INTERACTING F-BOX KELCH 1 (CFK1), whose orthologues were previously identified in 15 out of 18 plant species (Fig. S1a) (Hua *et al.*, 2011), as a potential candidate (Fig. 2a). CFK1 consists of a putative F-box domain at its N-terminus and two kelch repeats within its C-terminal substrate recognition domain (Fig. S1b). It has previously been shown to interact with Arabidopsis S-PHASE KINASE-ASSOCIATED PROTEIN 1-LIKE 1 (ASK1) to form an SCF ubiquitin ligase complex with two other subunits, Cullin 1 (CUL1) and Rbx1 (Zhao *et al.*, 2006; Franciosini *et al.*, 2013). To further verify this interaction, we examined its interaction with both ASK1 and ASK2, the two major SKP1 (S-phase kinase-associated protein 1) proteins in Arabidopsis (Liu *et al.*, 2004; Hua & Gao, 2019). Our yeast two-hybrid assay confirmed that CFK1 interacted with both ASK1 and ASK2 (Fig. 2a), suggesting that CFK1 is a bona fide F-box protein of a SCF protein complex.

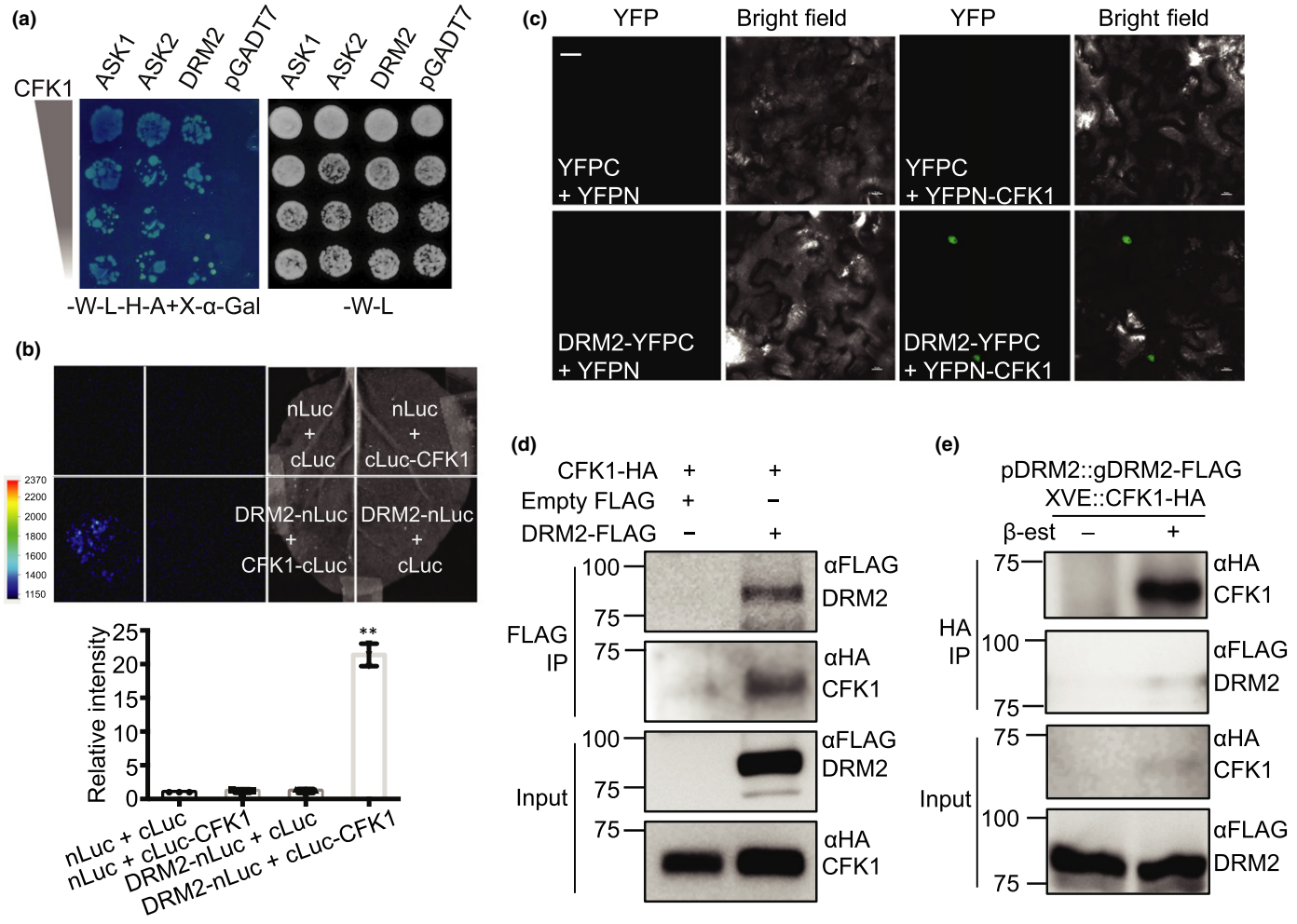

Fig. 2 COP9 SIGNALOSOME INTERACTING F-BOX KELCH 1 (CFK1) interacts with DOMAINS REARRANGED METHYLTRANSFERASE 2 (DRM2) *in vitro* and *in vivo*. (a) Interaction of CFK1 and DRM2 in a yeast two-hybrid assay. Empty vector pGADT7 was used as a negative control. ARABIDOPSIS SKIP1 HOMOLOGUE (ASK) 1 and ASK2 were used positive controls. −W−L−H−A + X-α-Gal indicates the dropout medium lacking adenine, histidine, leucine, and tryptophan, and supplemented with 5-bromo-4-chloro-3-indolyl-α-D-galactopyranoside (X-α-Gal). (b) Split luciferase (Luc) complementation assay showing the CFK1–DRM2 interaction. The indicated constructs were transiently co-expressed in *Nicotiana benthamiana*. The colour bar shows the range of luminescence intensity. The bar graph (lower panel) indicates the luminescence intensity relative to the control nLuc + cLuc. Error bars denote 2SD. Student's *t*-test, **, $P < 0.01$. (c) Interaction of CFK1 and DRM2 in *N. benthamiana* by bimolecular fluorescence complementation assay. Bar, 20 μm. CFK1 and DRM2 were fused to yellow fluorescent proteins (YFP)-N and YFP-C, respectively. The indicated constructs were transiently co-expressed in *N. benthamiana*. After 36–48 h, the YFP signal was visualised using a confocal microscope. (d) Co-immunoprecipitation of CFK1-HA and DRM2-FLAG in *N. benthamiana*. CFK1-HA was co-expressed with either DRM2-FLAG or empty vector in *N. benthamiana* by agroinfiltration. Samples were collected 2 d after infiltration. (e) Co-immunoprecipitation of CFK1-HA and DRM2-FLAG in transgenic Arabidopsis plants expressing both pDRM2::gDRM2-FLAG and XVE::CFK1-HA driven by an oestrogen receptor-based inducible system; 2 μM inducer β-oestradiol (β-est) was added in the half-strength Murashige and Skoog (½MS) medium to induce CFK1-HA protein expression.

To validate the interaction between CFK1 and DRM2, we performed a split luciferase (Luc) complementation assay by fusing DRM2 to N-terminal luciferase (DRM2-nLuc) and CFK1 to C-terminal luciferase (cLuc-CFK1). After co-inoculation in *N. benthamiana* leaves, luminescence was detected only with co-infiltrated DRM2-nLuc and cLuc-CFK1, but not with the negative controls DRM2-nLuc/cLuc and nLuc/cLuc-CFK1 (Fig. 2b). We also conducted a BiFC assay by fusing DRM2 to the C-terminal fragment of YFP (175-239, DRM2-YFPC) and CFK1 to the N-terminal part of YFP (1-173, YFPN-CFK1), and co-expressing them in *N. benthamiana* leaves. We detected positive fluorescence signals in the nuclei when co-inoculated YFPN-CFK1 and DRM2-YFPC, but not the negative vector controls (Fig. 2c), suggesting that DRM2 associated with CFK1. To further confirm the DRM2–CFK1 interaction *in vivo*, we performed a co-immunoprecipitation (Co-IP) experiment in *N. benthamiana* leaves co-expressing p35S::CFK1-HA and pDRM2::gDRM2-FLAG. Total protein was incubated with FLAG beads to immunoprecipitate DRM2-FLAG. The anti-HA antibody was used to detect immunoprecipitated proteins. CFK1-HA was detected in the DRM2–FLAG complex, but not in the empty FLAG vector control (Fig. 2d), confirming the interaction between DRM2 and CFK1. Additionally, we generated an estrogen receptor-based inducible system to transiently induce CFK1-HA overexpression in pDRM2::gDRM2-FLAG transgenic Arabidopsis plants and performed a reciprocal Co-IP assay. Total protein was incubated with HA antibody and Dynabeads protein G to immunoprecipitate CFK1-HA. The anti-FLAG antibody was used to detected immunoprecipitated proteins. DRM2-FLAG was detected in CFK1-HA complex (Fig. 2e), but not in the absence of estradiol induction control, further validating that DRM2 interacts with CFK1 *in vivo*. Consistent with our previous mass spectrometry data (Zhong *et al.*, 2014), we confirmed the interaction between DRM2 and ASK1 by both split luciferase and BiFC assays (Fig. S2a,b). Taken together, these results showed that DRM2 interacts with SCF^{CFK1} ubiquitin ligase through direct association with the F-box protein CFK1.

CFK1 degrades DRM2 protein

Given the DRM2–CFK1 interaction, we investigated whether CFK1 regulates DRM2 protein abundancy. First, we compared DRM2 protein levels in the presence or absence of CFK1 by transforming the pDRM2::gDRM2-HA plasmid into wild-type Col-0 or *cfk1* mutant protoplasts. Compared with wild-type Col-0 that has a functional CFK1, the DRM2 protein level was increased in *cfk1* mutants (Fig. 3a). Next, we checked the DRM2 protein abundance by overexpressing CFK1 in *N. benthamiana* leaves and noted a slight reduction in DRM2 levels when CFK1 was overexpressed compared with the control (Fig. 3b). The reduction of DRM2 protein was not observed when overexpressing HDA9, a negative control that does not regulate the stability of DRM2 (Fig. S3). To test whether CFK1 regulates DRM2 at the transcriptional level, we determined the *DRM2* mRNA transcript in *cfk1* mutant and found a similar RNA level as that of the wild-type (Fig. S4a). These results suggested that CFK1 negatively regulates DRM2 protein abundance. To further investigate the regulation of DRM2 by CFK1 *in planta*, we used an estrogen receptor-based inducible system to transiently induce CFK1 overexpression in pDRM2::gDRM2-FLAG transgenic Arabidopsis plants. Upon induction by β-estradiol, an inducer that regulates a chimeric transcription activator XVE, we noticed an elevated CFK1 protein level accompanied with a slightly reduced DRM2 protein level (Fig. 3c). Taken together, these data suggested that CFK1 degrades DRM2 protein *in planta*.

DRM2 is degraded through a CFK1-mediated proteasome pathway

We showed that DRM2 protein stability is regulated through the 26S proteasome and by CFK1. This prompted us to hypothesise that DRM2 is targeted for degradation through the SCF^{CFK1}-mediated proteasome pathway. To test this hypothesis, we generated stable DRM2-FLAG-tagged lines on the wild-type and *cfk1* mutant backgrounds (pDRM2::gDRM2-FLAG/WT and pDRM2::gDRM2-FLAG/*cfk1*) and examined the abundance of DRM2 protein after MG132 application. The knockout of *CFK1* gene in pDRM2::gDRM2-FLAG/*cfk1* was confirmed by genotyping PCR and RT-qPCR (Fig. S4b). To test whether the DRM2-FLAG transgene is functional, we transformed the same pDRM2::gDRM2-FLAG into the *drm1 drm2* (*dd*) mutant (termed pDRM2:gDRM2-FLAG/*dd*). We determined the ability of DRM2 transgene in rescuing *dd* mutant by examining the DNA methylation at a well known DRM2 target, *AtSN1*, by Chop-PCR. Three independent pDRM2:gDRM2-FLAG/*dd* T_1 transgenic lines showed successful rescues of the loss of DNA methylation as illustrated by visible bands after methylation sensitive enzyme *Hae*III digestion (Fig. S4c), suggesting that the DRM2 transgene is biologically functional.

Consistent with Fig. 1(a), DRM2 protein level was increased upon MG132 treatment in wild-type relative to mock treatment from two independent lines (Fig. 3d). By contrast, similar DRM2 protein levels were observed in the *cfk1* mutant with or without MG132 treatment (Fig. 3d). The difference in protein abundance was not due to transcriptional regulation, as similar *DRM2* mRNA levels were detected in pDRM2::gDRM2-FLAG/WT and pDRM2::gDRM2-FLAG/*cfk1* (Fig. S4d). To further confirm CFK1-mediated DRM2 degradation, we examined DRM2 protein stability in the *cfk1* mutant and wild-type by treatment with cycloheximide (CHX), a well known protein synthesis inhibitor (Jiang *et al.*, 2019). We found that DRM2 protein was decreased more rapidly in wild-type compared with *cfk1* (Figs 3e, S5). Taken together, these results suggested that DRM2 was degraded through the CFK1-mediated proteasome pathway.

CFK1 overexpression induces CHH hypomethylation and transcriptional de-repression at DRM2 target loci

DRM2 is a DNA methyltransferase predominantly acting on transposable elements (TEs) and repetitive DNA sequences to maintain genome stability in Arabidopsis (Zhong, 2016; Zhang *et al.*, 2018). To investigate the biological significance of CFK1-

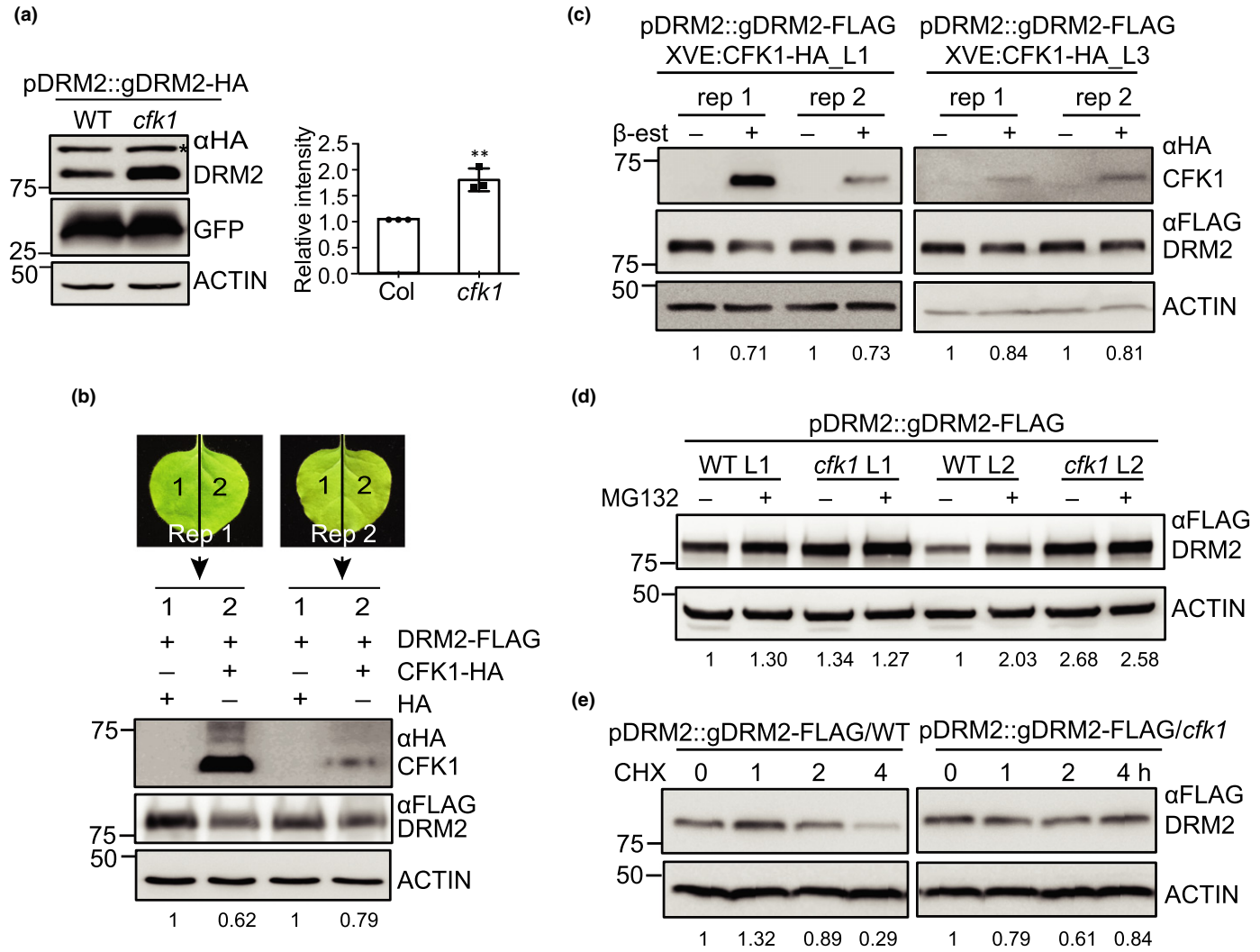

Fig. 3 DOMAINS REARRANGED METHYLTRANSFERASE 2 (DRM2) is degraded through a COP9 SIGNALOSOME INTERACTING F-BOX KELCH 1 (CFK1)-mediated proteasome pathway in Arabidopsis. (a) Immunoblot analysis showing the abundance of DRM2 protein transiently expressed in wild-type (WT) and *cfk1* mutant protoplasts. Empty green fluorescent protein (GFP) vector was co-transformed to monitor transfection efficiency. ACTIN was used as a loading control. * Indicates a nonspecific band. Bar graph (right) represents the average band intensity ratio of DRM2-HA to ACTIN from three biological replicates, measured using ImageJ software. Error bars denote 2SD, Student's *t*-test; **, $P < 0.01$. (b) Immunoblot analysis showing the abundance of DRM2-FLAG protein co-expressed with CFK1-HA in *N. benthamiana* from two biological replicates (Rep 1 and Rep 2). An HA empty vector was used as a negative control. Numbers indicate the relative band intensity ratio of DRM2-FLAG to ACTIN, measured by ImageJ software. (c) Immunoblot analysis showing DRM2 protein levels of two biological replicates (rep 1 and rep 2) in two independent transgenic plants (L1, left and L3, right) of pDRM2::gDRM2-FLAG XVE:CFK1-HA with β-oestradiol (β-est) treatment. Numbers indicate the relative band intensity ratio of DRM2-FLAG to ACTIN, measured by ImageJ software. (d) Immunoblot analysis showing DRM2 protein levels from two independent lines (L1 and L2) of pDRM2::gDRM2-FLAG/WT and pDRM2::gDRM2-FLAG/*cfk1* Arabidopsis transgenic seedlings treated with DMSO (–) or MG132 (+). Numbers indicate the relative band intensity ratio of DRM2-FLAG to ACTIN, quantified by ImageJ software. (e) Immunoblot analysis showing the half-life of DRM2 protein in pDRM2::gDRM2-FLAG/WT (left) and pDRM2::gDRM2-FLAG/*cfk1* (right) Arabidopsis transgenic seedlings treated with 500 μM cycloheximide (CHX) for the indicated time. ACTIN was used as a loading control. Numbers indicate the relative band intensity ratio of DRM2-FLAG to ACTIN, quantified by ImageJ software. This experiment was repeated three times. The other two biological replicates were shown in Supporting Information Fig. S5.

mediated DRM2 protein degradation, we determined the global DNA methylation by performing whole genome bisulfite sequencing (BS-seq) on Col-0, *drm2*, and two independent p35S::CFK1-FLAG overexpression lines (refer to CFK1 OE1 and CFK1 OE2) (Table S3). The *CFK1* mRNA level was increased 4–7 times in both OE lines and decent protein levels was detected compared with Col-0 (Fig. S6). We noticed a small but noticeable decrease in CHH methylation at the five Arabidopsis chromosomes in both CFK1 OE1 and OE2 lines (Figs 4a, S7a). The reduction is specific in the CHH context as no difference was noted in both CG and CHG methylation (Fig. S7a). Consistently, CHH methylation reduction was shown over the TE bodies, albeit to a lesser extent as *drm2* (Fig. 4b).

Next, we questioned whether CFK1 overexpression regulated locus-specific or genome-wide DNA methylation. To this end, we determined the DMRs in CFK1 OE1 and CFK1 OE2 and

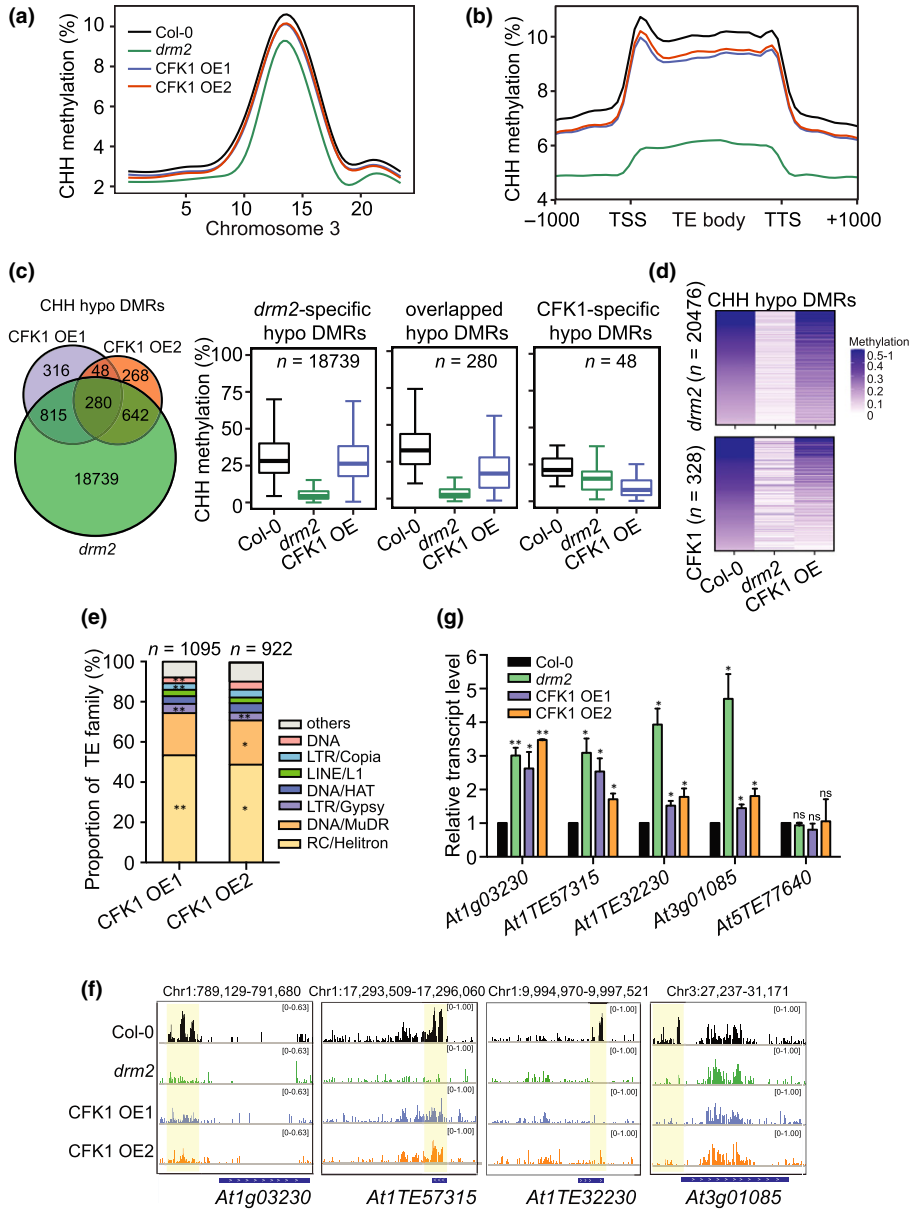

Fig. 4 COP9 SIGNALOSOME INTERACTING F-BOX KELCH 1 (CFK1) overexpression induces DNA hypomethylation and transcriptional de-repression at DOMAINS REARRANGED METHYLTRANSFERASE 2 (DRM2) target loci in Arabidopsis. (a) Metaplot showing average CHH methylation level of Col-0, *drm2*, and two p35S::CFK1-FLAG lines (CFK1 OE1 and CFK1 OE2) across chromosome 3. The numbers on the x-axis indicate the physical position at chromosome 3 in megabase (MB). The sliding window is 100 kilobase (kb) of 10 kb step size. (b) Metaplot showing average CHH methylation level of Col-0, *drm2*, CFK1 OE1 and OE2 over all TEs. (c) Venn diagrams showing the overlaps of CHH hypo DMRs between *drm2*, CFK1 OE1 and OE2. Boxplots showing average CHH methylation level at *drm2*-specific, CFK1-specific CHH hypo DMRs, and *drm2* and CFK1 OE1/2 overlapped CHH hypo DMRs. The centre line in the box indicates the median and box edges indicate the interquartile range (IQR) from the 25% to the 75% percentile. The whiskers denote ± 1.5 IQR. Mann–Whitney test: ***, $P < 0.001$. (d) Heat maps showing CHH methylation level over *drm2* (upper panel) and CFK1 OE1 and OE2 shared (lower panel) CHH hypo DMRs in Col-0, *drm2* and CFK1 OE. The colour scale indicates the range of CHH methylation level from 0 (white) to 1 (dark purple). (e) The proportion of the DMRs in CFK1 OE1 or OE2 overlapped with those in *drm2* in each TE family. Fisher's exact test, **, $P < 0.01$; *, $P < 0.05$. (f) Genome browser views of CHH methylation level at representative loci. (g) RT-qPCR of the corresponding target loci from (f). *At5TE77640* used as a negative control. Data represents mean 1SD. Student's *t*-test: *, $P < 0.05$; **, $P < 0.01$. ns, not significant.

found that the majority were hypo DMRs in CHH context, similar to *drm2* DMRs (Fig. S7b; Dataset S1). We identified a total of 1459 and 1238 CHH hypo DMRs in CFK1 OE1 and OE2 (Fig. S8a; Datasets S2, S3), respectively. It was noted that only a small subset of *drm2* DMRs overlapped with both CFK1 OE1 and OE2 (Figs 4c, S8a). This was consistent with our observation that the transient induction of CFK1 overexpression led to only 20–30% DRM2 protein reduction (Fig. 3c). The small decreased DRM2 protein abundance may be insufficient to cause DNA methylation reduction at all DRM2 genomic targets. Furthermore, additional components are likely to be involved in the regulation of DRM2 protein abundance, which is a dynamic

balance between the rate of protein synthesis and degradation (Varshavsky, 2017). Nevertheless, we found that 85% of hypo DMRs shared by CFK1 OE1 and OE2 (280 out of 328) overlapped with those of *drm2* (Fig. 4c). Specifically, 75% of CFK1 OE1 (1095 out of 1458 OE1) or CFK1 OE2 hypo DMRs (922 out of 1238 OE2) overlapped with those of *drm2*, respectively (Fig. S8a). Further analysis of CFK1-specific hypo DMRs revealed a significant reduction in CHH methylation in *drm2* mutant (Figs 4c,d, S8a), suggesting that these DMRs are likely to be the weak DRM2 targets. Most CFK1-specific hypo DMRs were located in TEs (Fig. S8b), which was similar to the major role of DRM2 in methylation of TEs. In addition, CFK1 preferentially targeted gene promoters and TEs (Fig. S8c), particularly those of RC/Helitron and DNA/MuDR families (Fig. 4e), consistent with those identified in *drm1 drm2* mutants by clustering analysis (Sasaki *et al.*, 2019). Further analysis of CHH methylation in the major three TE families, RC/Helitron, DNA/MuDR, and LTR-Gypsy, found a noticeable reduction in both CFK1 OE1 and OE2 lines (Fig. S8d), which was consistent with the overall TEs (Fig. 4b). Together, these data suggested that CFK1-mediated DRM2 protein degradation led to DNA hypomethylation resembling *drm2* to a lower degree.

Next, we investigated whether a reduction in CHH methylation at the DRM2 target loci was correlated with transcriptional changes. We examined the transcript levels of TEs and genic regions that had reduced CHH methylation in CFK1 OE1, OE2, and *drm2* (Fig. 4f) using quantitative RT-qPCR. The expression levels of *At1g03230, At1TE57315, At1TE32230* and *AT3G01085* were significantly elevated in both CFK1 OE lines, resembling a null *drm2* mutant (Fig. 4g). Taken together, these results suggested that CFK1 affected DRM2-mediated DNA methylation and transcription of DRM2 target loci.

Discussion

In this study, we investigated how a DNA methyltransferase was precisely regulated to ensure proper function, by focusing on its degradation process. The turnover of DRM2 protein within cells is important to establish and maintain a balanced level of DNA methylation. We identified CFK1, an F-box protein in the SCF E3 ligase complex, as a novel DRM2 interacting partner regulating DRM2 protein stability via the 26S proteasome pathway and DNA methylation status at DRM2 target loci (Fig. 5). In plants, the transcriptional regulation of ROS1, a DNA demethylase, by DNA methylation acted as a self-regulating epigenetic rheostat to ensure the balance between methylation and demethylation activities (Zhang *et al.*, 2018). Unlike most targets, *ROS1* transcription is promoted by DNA methylation within the promoter region regulated by the RdDM pathway, which in turn demethylates itself and other loci to control the overall level of DNA methylation (Williams *et al.*, 2015; Williams & Gehring, 2017). Here, we uncovered an additional layer of regulation by fine tuning the DRM2 protein at the post-translational level to control DNA methylation.

The mechanism underlying CFK1-mediated DNA methyltransferase reported in this study shares both similar and distinct features with that of UHRF1. In mammals, the *de novo* DNA methyltransferase DNMT3A is degraded by UHRF1/2 E3 ligase, as evidenced by decreased DNMT3A protein levels in UHRF1/2 overexpression, and consequently results in DNA hypomethylation (Jia *et al.*, 2016). Consistently, the transient CFK1 induction results in a reduced DRM2 protein level, which then leads to the DNA methylation change at some DRM2 target loci in Arabidopsis. UHRF1 is well characterised for its role as a ubiquitin E3 ligase of DNMT1 in regulating DNA methylation maintenance (Du *et al.*, 2010). However, it is unlikely that CFK1 is involved in regulating MET1 (DNMT1 homologue in Arabidopsis)-mediated CG methylation maintenance because CFK1 lacks SRA domain, which is present in UHRF1 that binds to hemi-methylated DNA and recruits DNMT1 (Bostick *et al.*, 2007). We found that the global CG methylation level was unchanged when overexpressing CFK1 (Fig. S7a). Also, VIM proteins, homologues of UHRF1 in Arabidopsis, have been reported to be functional ubiquitin E3 ligases and are implicated in the maintenance of CG DNA methylation in cooperation with MET1 (Feng *et al.*, 2010; Kim *et al.*, 2014). Therefore, our results suggested that CFK1 may be a plant-specific E3 ligase for DRM2.

CFK1 was previously identified as an F-box protein of SCF E3 ubiquitin ligase complex (Franciosini *et al.*, 2013). Consistently, we also found that CFK1 interacted with ASK1 (Fig. 2a), a predominant Arabidopsis SKP1 protein that binds F-box proteins (Hua & Vierstra, 2011). F-box proteins recognise target proteins and facilitate the ubiquitin transfer from E2 ubiquitin conjugating enzymes to substrates (Kipreos & Pagano, 2000; Hua & Vierstra, 2011; Skaar *et al.*, 2014). A 76-amino-acid ubiquitin was added sequentially to the target protein as a signal for proteasome degradation (Vierstra, 1993; Marshall & Vierstra, 2019). We postulated that CFK1 regulated the poly-ubiquitination of DRM2. Despite extensive efforts, we were unable to detect the ubiquitination level change of DRM2 between *cfk1* knockout mutants and wild-type Col-0 plants. One possible reason is that endogenous F-box proteins are unstable and subject to SCF-mediated ubiquitination (Zhou & Howley, 1998). It has been shown that CFK1 stability itself is regulated by proteasome-dependent proteolysis (Franciosini *et al.*, 2013). Another possible reason is that ubiquitin-dependent protein degradation is enhanced by small molecules. For example, plant hormone auxin, responsive to environmental stimuli, induces the degradation of transcriptional repressor AUX/IAA by functioning as a 'molecular glue' to enhance the interaction between F-box protein TIR1 and AUX/IAA (Tan & Zheng, 2009). Our experiments were performed under normal conditions, which could also explain why we observed a low fold change at DRM2 protein levels in loss-of-function *CFK1* (Fig. 3). Therefore, identification of signals that enhance CFK1-DRM2 interaction may provide further insights into CFK1-mediated ubiquitination and degradation of DRM2.

DRM2 is responsible for *de novo* DNA methylation and maintenance CHH methylation (Cao & Jacobsen, 2002; Cao *et al.*, 2003). Mutation in DRM2 results in DNA hypomethylation (Stroud *et al.*, 2013). Here, we also detected a global reduction of CHH DNA methylation level in CFK1 overexpression lines that

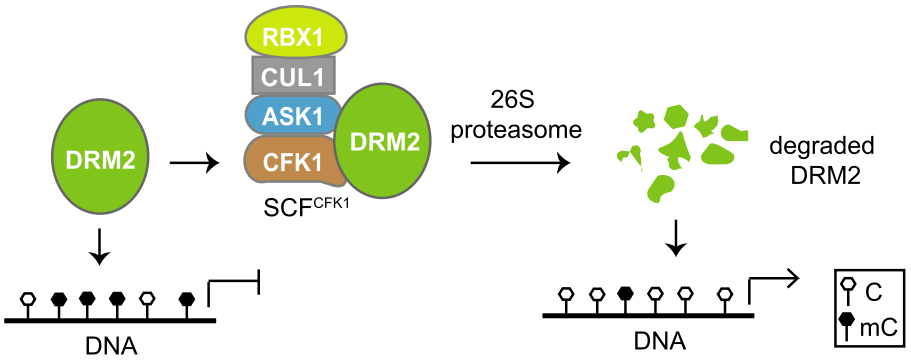

Fig. 5 A model for COP9 SIGNALOSOME INTERACTING F-BOX KELCH 1 (CFK1)-mediated DOMAINS REARRANGED METHYLTRANSFERASE 2 (DRM2) degradation and hypomethylation in Arabidopsis. DRM2 associates with the SCF^{CFK1} complex consisting of RING-box protein-1 (RBX1), Cullin-1 (CUL1), Arabidopsis S-phase-kinase-associated protein-1 (Skp1) Homologue 1 (ASK1), and F-box protein CFK1, through ASK1 (previously published data) and CFK1 (this study). CFK1 interacts and targets DRM2 for degradation through ubiquitin-26S proteasome. Consequently, the reduced DRM2 protein abundance results in hypomethylation and transcriptional de-repression at some DRM2 target loci.

have reduced DRM2 protein levels (Figs 4a, S7a). Increased DRM2 protein abundance in *cfk1* mutants is expected to induce DNA hypermethylation. However, we did not detect increased DNA methylation in *cfk1* mutants at the three well characterised RdDM targets *AtSN1, AtMu1* and *Cluster 4* (Fig. S9). A possible explanation is that additional small increases within already highly methylated loci are challenging to be detected. Similarly, only a 0.25% increase in 5-mC methylation was detected in mouse embryonic carcinoma cells after knocking down UHRF2 (E3 ligase of DNMT3A) (Jia *et al.*, 2016). It has been reported that CFK2 showed a high sequence similarity with CFK1 and shared functional redundancy with CFK1 in the promotion of the hypocotyl length under red and far-red light (Franciosini *et al.*, 2013). It is possible that knocking out CFK1 alone did not cause hypermethylation at the tested loci, *AtSN1, AtMu1* and *Cluster 4*. Further experiments could be carried out on double mutants *cfk1 cfk2* to test whether those loci are hypermethylated. Besides the three tested loci, it would be interesting to check whether there is any *de novo* methylation at naïve loci, for instance, newly inserted TEs, in *cfk1* mutant.

UBA domain was first identified to be associated with ubiquitination and has been implicated in proteasomal degradation (Su & Lau, 2009). DRM2 has three UBA domains, which were previously characterised to be required for genome-wide DRM2 activity, as mutation of the UBA domains led to the global loss of DNA methylation (Zhong *et al.*, 2014). Given this finding, we wondered whether UBA domains influenced DRM2 ubiquitination and degradation to control DNA methylation. If UBA domains are important for CFK1-mediated DRM2 degradation, then mutation of the aUBA domain would prevent DRM2 from ubiquitination and degradation, thus leading to an increased DRM2 protein abundance. However, a previous study showed that mutation in the UBA domains did not affect the overall DRM2 protein levels (Zhong *et al.*, 2014). Therefore, UBA domains are most likely not involved in CFK1-mediated DRM2 degradation.

DNA methylation and repressive histone marks, H3K9me, are highly correlated with gene silencing (Du *et al.*, 2015). Recent studies revealed that the RING motif of JMJ24, instead of the JmjC domain that is well characterised with histone demethylase activity (Klose *et al.*, 2006; Deng *et al.*, 2016), is required for regulating CHG methylation and H3K9me2, to reinforce transcriptional silencing (Klose *et al.*, 2006; Deng *et al.*, 2016; Kabelitz *et al.*, 2016). Rbx1, the core subunit in SCF complex, contains the RING domain (Gray *et al.*, 2002; Zheng *et al.*, 2002). Therefore, it would be interesting to investigate whether SCF^{CFK1} also regulates the histone methylation, which could provide further insights into DRM2-mediated DNA methylation and histone modifications.

The ubiquitin-mediated degradation system plays a vital role in removing abnormal proteins that arise during stress conditions to maintain cellular homeostasis and growth (Flick & Kaiser, 2012; Sharma *et al.*, 2016). It has been reported that DNA methylation is involved in the stress response. DNA methylation mutants *met1* and *drm1 drm2 cmt3* (*ddc*) displayed enhanced resistance to *Pseudomonas syringae* pv. *tomato* DC3000 infection (Dowen *et al.*, 2012; McKown *et al.*, 2014). Various abiotic and biotic stress factors can lead to dynamic changes in DNA methylation (Thiebaut *et al.*, 2019). For instance, centromeric repeats in wild-type were hypomethylated after *Pst* infection (Pavet *et al.*, 2007). It would be interesting to investigate whether SCF^{CFK1}-mediated DRM2 degradation also plays a role in the stress response. Findings from such studies may shed light on how plants respond to environmental stimuli through epigenetic regulation. It has been shown that DRM2 is responsible for establishing sexual-lineage hypermethylated loci in male meiocytes through RdDM pathway (Walker *et al.*, 2017). An early study indicated that the meiocytes of *ask1* mutants had altered chromatin structure, accompanied with alterations in prolonged telomere attachment to the nucleolus and modified histones (Yang, 2006). As CFK1 has been shown to associate with ASK1, it raised the possibility that CFK1-mediated DRM2 degradation may play an important role in sexual-lineage development in plants.

Acknowledgements

We would like to thank Professors Richard Vierstra at Washington University in St Louis for the ubiquitin antibody and Nam-

Hai Chua at Rockefeller University for the β-estradiol-inducible pER8 vector. We thank Professor Ning Zheng at the University of Washington for valuable suggestions. Work in the Zhong laboratory was supported by a NSF CAREER award (MCB-1552455), NIH-MIRA (R35GM124806), and USDA & National Institute of Food and Agriculture grant (Hatch 1012915) and work in the Hua laboratory was supported by a NSF CAREER award (MCB-1750361).

Author contributions

JC and XZ designed this study. JC performed most of the experiments unless indicated as follows. SQ and JJ provided DRM2 construct in the pGAD-T7 vector. JL performed BS-sequencing data analysis. JS and ZH carried out the yeast two-hybrid assay. JJ performed the confocal microscopy in the BiFC assay. JC, RK and ID generated CFK1-FLAG and DRM2-FLAG-tagged lines. GS and FL provided technical support. JC and XZ interpreted the results and wrote the manuscript with input from coauthors.

ORCID

Jiani Chen https://orcid.org/0000-0003-3785-7289
Zhihua Hua https://orcid.org/0000-0003-1177-1612
Jianjun Jiang https://orcid.org/0000-0003-3887-2624
Fengquan Liu https://orcid.org/0000-0001-9325-1500
Jie Liu https://orcid.org/0000-0002-1129-9584
Shuiming Qian https://orcid.org/0000-0002-8510-3863
Giovanna Serino https://orcid.org/0000-0001-8689-6132
Xuehua Zhong https://orcid.org/0000-0002-2350-0046

Data availability

All sequencing data used in this study are available under NCBI GEO accession number (GSE148553).

References

Augustine RC, Vierstra RD. 2018. SUMOylation: re-wiring the plant nucleus during stress and development. *Current Opinion in Plant Biology* **45**: 143–154.

Azevedo J, Picart C, Dureau L, Pontier D, Jaquinod-Kieffer S, Hakimi MA, Lagrange T. 2019. UAP56 associates with DRM2 and is localized to chromatin in Arabidopsis. *FEBS Open Bio* **9**: 973–985.

Baets J, Duan X, Wu Y, Smith G, Seeley WW, Mademan I, McGrath NM, Beadell NC, Khoury J, Botuyan MV *et al.* 2015. Defects of mutant DNMT1 are linked to a spectrum of neurological disorders. *Brain* **138**: 845–861.

Bird A. 2002. DNA methylation patterns and epigenetic memory. *Genes & Development* **12**: 47–56.

Bolger AM, Lohse M, Usadel B. 2014. Trimmomatic: a flexible trimmer for Illumina sequence data. *Bioinformatics* **30**: 2114–2120.

Bostick M, Kim J, Esteve P, Clark A, Pradhan S, Jacobsen S. 2007. UHRF1 plays a role in maintaining DNA methylation in Mammalian cells. *Science* **317**: 1760–1764.

Cao X, Aufsatz W, Zilberman D, Mette MF, Huang MS, Matzke M, Jacobsen SE. 2003. Role of the DRM and CMT3 methyltransferases in RNA-directed DNA methylation. *Current Biology* **13**: 2212–2217.

Cao X, Jacobsen S. 2002. Role of the *Arabidopsis DRM* methyltransferases in de novo DNA methylation and gene silencing. *Current Biology* **12**: 1138–1144.

Chan SW, Henderson IR, Zhang X, Shah G, Chien JS, Jacobsen SE. 2006. RNAi, DRD1, and histone methylation actively target developmentally important non-CG DNA methylation in *Arabidopsis*. *PLoS Genetics* **2**: e83.

Chen JN, Nolan TM, Ye HX, Zhang MC, Tong HN, Xin PY, Chu JF, Chu CC, Li ZH, Yin YH. 2017. Arabidopsis WRKY46, WRKY54, and WRKY70 transcription factors are involved in brassinosteroid-regulated plant growth and drought responses. *The Plant Cell* **29**: 1425–1439.

Chen X, Lu L, Mayer KS, Scalf M, Qian S, Lomax A, Smith LM, Zhong X. 2016. POWERDRESS interacts with HISTONE DEACETYLASE 9 to promote aging in Arabidopsis. *eLife* **5**: e17214.

Chen X, Lu L, Qian S, Scalf M, Smith LM, Zhong X. 2018. Canonical and noncanonical actions of Arabidopsis histone deacetylases in ribosomal RNA processing. *The Plant Cell* **30**: 134–152.

Clough SJ, Bent AF. 1998. Floral dip: a simplified method for Agrobacterium-mediated transformation of *Arabidopsis thaliana*. *The Plant Journal* **16**: 735–743.

Deng S, Jang IC, Su L, Xu J, Chua NH. 2016. JMJ24 targets CHROMOMETHYLASE3 for proteasomal degradation in *Arabidopsis*. *Genes & Development* **30**: 251–256.

Denis H, Ndlovu MN, Fuks F. 2011. Regulation of mammalian DNA methyltransferases: a route to new mechanisms. *EMBO Reports* **12**: 647–656.

Deplus R, Blanchon L, Rajavelu A, Boukaba A, Defrance M, Luciani J, Rothe F, Dedeurwaerder S, Denis H, Brinkman AB *et al.* 2014. Regulation of DNA methylation patterns by CK2-mediated phosphorylation of Dnmt3a. *Cell Reports* **8**: 743–753.

Dowen RH, Pelizzola M, Schmitz RJ, Lister R, Dowen JM, Nery JR, Dixon JE, Ecker JR. 2012. Widespread dynamic DNA methylation in response to biotic stress. *Proceedings of the National Academy of Sciences, USA* **109**: E2183–E2191.

Du J, Johnson LM, Jacobsen SE, Patel DJ. 2015. DNA methylation pathways and their crosstalk with histone methylation. *Nature Reviews Molecular Cell Biology* **16**: 519–532.

Du Z, Song J, Wang Y, Zhao Y, Guda K, Yang S, Kao HY, Xu Y, Willis J, Markowitz SD *et al.* 2010. DNMT1 stability is regulated by proteins coordinating deubiquitination and acetylation-driven ubiquitination. *Science Signaling* **3**: ra80.

Edgar RC. 2004. MUSCLE: multiple sequence alignment with high accuracy and high throughput. *Nucleic Acids Research* **32**: 1792–1797.

Esteve PO, Chang Y, Samaranayake M, Upadhyay AK, Horton JR, Feehery GR, Cheng X, Pradhan S. 2011. A methylation and phosphorylation switch between an adjacent lysine and serine determines human DNMT1 stability. *Nature Structural & Molecular Biology* **18**: 42–48.

Feng S, Cokus SJ, Zhang X, Chen PY, Bostick M, Goll MG, Hetzel J, Jain J, Strauss SH, Halpern ME *et al.* 2010. Conservation and divergence of methylation patterning in plants and animals. *Proceedings of the National Academy of Sciences, USA* **107**: 8689–8694.

Flick K, Kaiser P. 2012. Protein degradation and the stress response. *Seminars in Cell & Developmental Biology* **23**: 515–522.

Franciosini A, Lombardi B, Iafrate S, Pecce V, Mele G, Lupacchini L, Rinaldi G, Kondou Y, Gusmaroli G, Aki S *et al.* 2013. The Arabidopsis COP9 SIGNALOSOME INTERACTING F-BOX KELCH 1 protein forms an SCF ubiquitin ligase and regulates hypocotyl elongation. *Molecular Plant* **6**: 1616–1629.

Garzon RLS, Fabbri M, Liu Z, Heaphy CE, Callegari E, Schwind S, Pang J, Yu J, Muthusamy N, Havelange V *et al.* 2009. MicroRNA-29b induces global DNA hypomethylation and tumor suppressor gene reexpression in acute myeloid leukemia by targeting directly DNMT3A and 3B and indirectly DNMT1. *Blood* **113**: 6411–6418.

Gray WM, Hellmann H, Dharmasiri S, Estelle M. 2002. Role of the Arabidopsis RING-H2 protein RBX1 in RUB modification and SCF function. *The Plant Cell* **14**: 2137–2144.

Guo H, Nolan TM, Song G, Liu S, Xie Z, Chen J, Schnable PS, Walley JW, Yin Y. 2018. FERONIA receptor kinase contributes to plant immunity by suppressing jasmonic acid signaling in *Arabidopsis thaliana*. *Current Biology* **28**: 3316–3324 e3316.

Henderson IR, Jacobsen SE. 2008. Tandem repeats upstream of the Arabidopsis endogene SDC recruit non-CG DNA methylation and initiate siRNA spreading. *Genes & Development* **22**: 1597–1606.

Henderson IR, Wong W, Zhong X, Chin HG, Horwitz GA, Kelly KA, Pradhan S, Jacobsen SE. 2010. The *de novo* cytosine methyltransferase DRM2 requires intact UBA domains and a catalytically mutated paralog DRM3 during RNA-directed DNA methylation in *Arabidopsis thaliana*. *PLoS Genetics* **6**: 1001182.

Hervouet E, Lalier L, Debien E, Cheray M, Geairon A, Rogniaux H, Loussouarn D, Martin SA, Vallette FM, Cartron PF. 2010. Disruption of Dnmt1/PCNA/UHRF1 interactions promotes tumorigenesis from human and mice glial cells. *PLoS ONE* **5**: e11333.

Hua Z, Early MJ. 2019. Closing target trimming and CTTdocker programs for discovering hidden superfamily loci in genomes. *PLoS ONE* **14**: e0209468.

Hua Z, Gao Z. 2019. Adaptive and degenerative evolution of the S-Phase Kinase-Associated Protein 1-Like family in *Arabidopsis thaliana*. *PeerJ* **7**: e6740.

Hua Z, Pool JE, Schmitz RJ, Schultz MD, Shiu SH, Ecker JR, Vierstra RD. 2013. Epigenomic programming contributes to the genomic drift evolution of the F-Box protein superfamily in *Arabidopsis*. *Proceedings of the National Academy of Sciences, USA* **110**: 16927–16932.

Hua Z, Vierstra RD. 2011. The cullin-RING ubiquitin-protein ligases. *Annual Review of Plant Biology* **62**: 299–334.

Hua Z, Zou C, Shiu SH, Vierstra RD. 2011. Phylogenetic comparison of F-Box (FBX) gene superfamily within the plant kingdom reveals divergent evolutionary histories indicative of genomic drift. *PLoS ONE* **6**: e16219.

Jha A, Shankar R. 2014. miRNAting control of DNA methylation. *Journal of Biosciences* **39**: 365–380.

Jia S, Kobayashi R, Grewal SI. 2005. Ubiquitin ligase component Cul4 associates with Clr4 histone methyltransferase to assemble heterochromatin. *Nature Cell Biology* **7**: 1007–1013.

Jia Y, Li P, Fang L, Zhu H, Xu L, Cheng H, Zhang J, Li F, Feng Y, Li Y *et al.* 2016. Negative regulation of DNMT3A de novo DNA methylation by frequently overexpressed UHRF family proteins as a mechanism for widespread DNA hypomethylation in cancer. *Cell Discovery* **2**: 16007.

Jiang H, Tang BY, Xie ZL, Nolan T, Ye HX, Song GY, Walley J, Yin YH. 2019. GSK3-like kinase BIN2 phosphorylates RD26 to potentiate drought signaling in Arabidopsis. *The Plant Journal* **100**: 923–937.

Jin ZL, Liu Y. 2018. DNA methylation in human diseases. *Genes & Diseases* **5**: 1–8.

Kabelitz T, Brzezinka K, Friedrich T, Górka M, Graf A, Kappel C, Bäurle I. 2016. A JUMONJI protein with E3 ligase and histone H3 binding activities affects transposon silencing in Arabidopsis. *Plant Physiology* **171**: 344–358.

Kim J, Kim JH, Richards EJ, Chung KM, Woo HR. 2014. Arabidopsis VIM proteins regulate epigenetic silencing by modulating DNA methylation and histone modification in cooperation with MET1. *Molecular Plant* **7**: 1470–1485.

Kipreos E, Pagano M. 2000. The F-box protein family. *Genome Biology* **1**: 3002.3001–3002.3007.

Klose RJ, Kallin EM, Zhang Y. 2006. JmjC-domain-containing proteins and histone demethylation. *Nature Reviews Genetics* **7**: 715–727.

Lavoie G, St-Pierre Y. 2011. Phosphorylation of human DNMT1: implication of cyclin-dependent kinases. *Biochemical and Biophysical Research Communications* **409**: 187–192.

Law JA, Jacobsen SE. 2010. Establishing, maintaining and modifying DNA methylation patterns in plants and animals. *Nature Reviews Genetics* **11**: 204–220.

Li H, Handsaker B, Wysoker A, Fennell T, Ruan J, Homer N, Marth G, Abecasis G, Durbin R, 1000 Genome Project Data Processing Subgroup. 2009. The sequence Alignment/Map format and SAMtools. *Bioinformatics* **25**: 2078–2079.

Li L. 2003. OrthoMCL: identification of ortholog groups for eukaryotic genomes. *Genome Research* **13**: 2178–2189.

Liu F, Ni W, Griffith ME, Huang Z, Chang C, Peng W, Ma H, Xie D. 2004. The *ASK1* and *ASK2* genes are essential for Arabidopsis early development. *The Plant Cell* **16**: 5–20.

Marshall RS, Vierstra RD. 2019. Dynamic regulation of the 26S proteasome: from synthesis to degradation. *Frontiers in Molecular Biosciences* **6**: 40.

Matzke MA, Kanno T, Matzke AJ. 2015. RNA-directed DNA methylation: the evolution of a complex epigenetic pathway in flowering plants. *Annual Review of Plant Biology* **66**: 243–267.

Matzke MA, Mosher RA. 2014. RNA-directed DNA methylation: an epigenetic pathway of increasing complexity. *Nature Reviews Genetics* **15**: 394–408.

McKown AD, Guy RD, Quamme L, Klapste J, La Mantia J, Constabel CP, El-Kassaby YA, Hamelin RC, Zifkin M, Azam MS. 2014. Association genetics, geography and ecophysiology link stomatal patterning in Populus trichocarpa with carbon gain and disease resistance trade-offs. *Molecular Ecology* **23**: 5771–5790.

Mosher RA, Schwach F, Studholme D, Baulcombe DC. 2008. PolIVb influences RNA-directed DNA methylation independently of its role in siRNA biogenesis. *Proceedings of the National Academy of Sciences, USA* **105**: 3145–3150.

Myung J, Kim K, Crews C. 2001. The ubiquitin-proteasome pathway and proteasome inhibitors. *Medicinal Research Reviews* **21**: 245–273.

Nishiyama A, Yamaguchi L, Sharif J, Johmura Y, Kawamura T, Nakanishi K, Shimamura S, Arita K, Kodama T, Ishikawa F *et al.* 2013. Uhrf1-dependent H3K23 ubiquitylation couples maintenance DNA methylation and replication. *Nature* **502**: 249–253.

Nolan TM, Brennan B, Yang M, Chen J, Zhang M, Li Z, Wang X, Bassham DC, Walley J, Yin Y. 2017. Selective autophagy of BES1 mediated by DSK2 balances plant growth and survival. *Developmental Cell* **41**: 33–46 e37.

Norvil AB, Saha D, Dar MS, Gowher H. 2019. Effect of disease-associated germline mutations on structure function relationship of DNA methyltransferases. *Genes* **10**: 1–16.

Okano M, Bell D, Haber D, Li E. 1999. DNA Methyltransferases Dnmt3a and Dnmt3b are essential for de novo methylation and mammalian development. *Cell* **99**: 247–257.

Pavet V, Quintero C, Cecchini NM, Rosa AL, Alvarez ME. 2007. *Arabidopsis* displays centromeric DNA hypomethylation and cytological alterations of heterochromatin upon attack by *Pseudomonas syringae*. *Molecular Plant–Microbe Interactions* **19**: 577–587.

Pignatta D, Bell GW, Gehring M. 2015. Whole genome bisulfite sequencing and DNA methylation analysis from plant tissue. *Bio-protocol* **5**: 1–16.

Pikaard CS, Mittelsten Scheid O. 2014. Epigenetic regulation in plants. *Cold Spring Harbor Perspectives in Biology* **6**: a019315.

Qin W, Wolf P, Liu N, Link S, Smets M, La Mastra F, Forne I, Pichler G, Horl D, Fellinger K *et al.* 2015. DNA methylation requires a DNMT1 ubiquitin interacting motif (UIM) and histone ubiquitination. *Cell Research* **25**: 911–929.

Quinlan AR. 2014. BEDTools: the swiss-army tool for genome feature analysis. *Current Protocols Bioinformatics* **8**: 1–34.

Raasi S, Varadan R, Fushman D, Pickart CM. 2005. Diverse polyubiquitin interaction properties of ubiquitin-associated domains. *Nature Structural & Molecular Biology* **12**: 708–714.

Ramirez F, Dundar F, Diehl S, Gruning BA, Manke T. 2014. deepTools: a flexible platform for exploring deep-sequencing data. *Nucleic Acids Research* **42** (Web Server issue): W187–W191.

Robertson KD, Wolffe AP. 2000. DNA methylation in health and disease. *Nature Reviews Genetics* **1**: 11–19.

Sasaki E, Kawakatsu T, Ecker JR, Nordborg M. 2019. Common alleles of *CMT2* and *NRPE1* are major determinants of CHH methylation variation in *Arabidopsis thaliana*. *PLoS Genetics* **15**: e1008492.

Sharma B, Joshi D, Yadav PK, Gupta AK, Bhatt TK. 2016. Role of ubiquitin-mediated degradation system in plant biology. *Frontiers in Plant Science* **7**: 806.

Skaar JR, Pagan JK, Pagano M. 2014. SCF ubiquitin ligase-targeted therapies. *Nature Reviews Drug Discovery* **13**: 889–903.

Sridhar VV, Kapoor A, Zhang K, Zhu J, Zhou T, Hasegawa PM, Bressan RA, Zhu JK. 2007. Control of DNA methylation and heterochromatic silencing by histone H2B deubiquitination. *Nature* **447**: 735–738.

Stamatakis A. 2014. RAxML version 8: a tool for phylogenetic analysis and post-analysis of large phylogenies. *Bioinformatics* **30**: 1312–1313.

Stroud H, Greenberg MV, Feng S, Bernatavichute YV, Jacobsen SE. 2013. Comprehensive analysis of silencing mutants reveals complex regulation of the Arabidopsis methylome. *Cell* **152**: 352–364.

Su V, Lau AF. 2009. Ubiquitin-like and ubiquitin-associated domain proteins: significance in proteasomal degradation. *Cellular and Molecular Life Sciences* **66**: 2819–2833.

Tan X, Zheng N. 2009. Hormone signaling through protein destruction: a lesson from plants. *American Journal of Physiology. Endocrinology and Metabolism* **296**: E223–227.

Thiebaut F, Hemerly AS, Ferreira PCG. 2019. A role for epigenetic regulation in the adaptation and stress responses of non-model plants. *Frontiers in Plant Science* **10**: 1–7.

Thompson JJ, Robertson KD. 2017. Misregulation of DNA methylation regulators in cancer. In: Kaneda A, Tsukada Y eds. *DNA and histone methylation as cancer targets. Cancer drug discovery and development*. Cham, Switzerland: Humana Press, 97–124.

Varshavsky A. 2017. The ubiquitin system, autophagy, and regulated protein degradation. *Annual Review of Biochemistry* **86**: 123–128.

Vierstra R. 1993. Protein degradation in plants. *Annual Review of Plant Physiology and Plant Molecular Biology* **44**: 385–410.

Vierstra R. 2003. The ubiquitin/26S proteasome pathway, the complex last chapter in the life of many plant proteins. *Trends in Plant Science* **8**: 135–142.

Walker J, Gao H, Zhang J, Aldridge B, Vickers M, Higgins JD, Feng X. 2017. Sexual-lineage-specific DNA methylation regulates meiosis in *Arabidopsis*. *Nature Genetics* **50**: 130–137.

Weber M, Schubeler D. 2007. Genomic patterns of DNA methylation: targets and function of an epigenetic mark. *Current Opinion in Cell Biology* **19**: 273–280.

Wendte JM, Schmitz RJ. 2018. Specifications of targeting heterochromatin modifications in plants. *Molecular Plant* **11**: 381–387.

Williams BP, Gehring M. 2017. Stable transgenerational epigenetic inheritance requires a DNA methylation-sensing circuit. *Nature Communications* **8**: 2124.

Williams BP, Pignatta D, Henikoff S, Gehring M. 2015. Methylation-sensitive expression of a DNA demethylase gene serves as an epigenetic rheostat. *PLoS Genetics* **11**: e1005142.

Xi Y, Li W. 2009. BSMAP: whole genome bisulfite sequence MAPping program. *BMC Bioinformatics* **10**: 232.

Xie Z, Johansen LK, Gustafson AM, Kasschau KD, Lellis AD, Zilberman D, Jacobsen SE, Carrington JC. 2004. Genetic and functional diversification of small RNA pathways in plants. *PLoS Biology* **2**: E104.

Yang X. 2006. The Arabidopsis *SKP1* homolog *ASK1* controls meiotic chromosome remodeling and release of chromatin from the nuclear membrane and nucleolus. *Journal of Cell Science* **119**: 3754–3763.

Yang Z, Qian S, Scheid RN, Lu L, Chen X, Liu R, Du X, Lv X, Boersma MD, Scalf M *et al.* 2018. EBS is a bivalent histone reader that regulates floral phase transition in *Arabidopsis*. *Nature Genetics* **50**: 1247–1253.

Yoo SD, Cho YH, Sheen J. 2007. *Arabidopsis* mesophyll protoplasts: a versatile cell system for transient gene expression analysis. *Nature Protocols* **2**: 1565–1572.

Zhang H, Lang Z, Zhu JK. 2018. Dynamics and function of DNA methylation in plants. *Nature Reviews Molecular Cell Biology* **19**: 489–506.

Zhao D, Yang X, Quan L, Timofejeva L, Rigel NW, Ma H, Makaroff CA. 2006. *ASK1*, a *SKP1* homolog, is required for nuclear reorganization, presynaptic homolog juxtaposition and the proper distribution of cohesin during meiosis in *Arabidopsis*. *Plant Molecular Biology* **62**: 99–110.

Zhao Y, Shen Y, Yang S, Wang J, Hu Q, Wang Y, He Q. 2010. Ubiquitin ligase components Cullin4 and DDB1 are essential for DNA methylation in *Neurospora crassa*. *Journal of Biological Chemistry* **285**: 4355–4365.

Zheng N, Schulman B, Song L, Miller J, Jeffrey P, Wang P, Chu C, Koepp D, Elledge S, Pagano M *et al.* 2002. Structure of the Cul1–Rbx1–Skp1–FboxSkp2 SCF ubiquitin ligase complex. *Nature* **416**: 703–709.

Zhong X. 2016. Comparative epigenomics: a powerful tool to understand the evolution of DNA methylation. *New Phytologist* **210**: 76–80.

Zhong X, Du J, Hale CJ, Gallego-Bartolome J, Feng S, Vashisht AA, Chory J, Wohlschlegel JA, Patel DJ, Jacobsen SE. 2014. Molecular mechanism of action of plant DRM De Novo DNA methyltransferases. *Cell* **157**: 1050–1060.

Zhong X, Hale CJ, Nguyen M, Ausin I, Groth M, Hetzel J, Vashisht AA, Henderson IR, Wohlschlegel JA, Jacobsen SE. 2015. Domains rearranged methyltransferase3 controls DNA methylation and regulates RNA polymerase V transcript abundance in *Arabidopsis*. *Proceedings of the National Academy of Sciences, USA* **112**: 911–916.

Zhou P, Howley P. 1998. Ubiquitination and degradation of the substrate recognition subunits of SCF ubiquitin-protein ligases. *Molecular Cell* **2**: 571–580.

Zilberman D, Cao X, Jacobsen SE. 2003. ARGONAUTE4 control of locus-specific siRNA accumulation and DNA and histone methylation. *Science* **299**: 716–719.

Zuo J, Niu QW, Chua NH. 2000. An estrogen receptor-based transactivator XVE mediateshighly inducible gene expression in transgenic plants. *The Plant Journal* **24**: 265–273.

Supporting Information

Additional Supporting Information may be found online in the Supporting Information section at the end of the article.

Data set S1 Differentially methylated regions (DMRs) in the *drm2* mutant.

Data set S2 Differentially methylated regions (DMRs) in CFK1 OE1.

Data set S3 Differentially methylated regions (DMRs) in CFK1 OE2.

Fig. S1 Phylogenetic tree of COP9 SIGNALOSOME INTERACTING F-BOX KELCH 1 (CFK1) subfamily.

Fig. S2 DOMAINS REARRANGED METHYLTRANSFERASE 2 (DRM2) interacts with ARABIDOPSIS SKIP1 HOMOLOGUE 1 (ASK1) *in vivo*.

Fig. S3 Immunoblot analysis showing the abundance of DOMAINS REARRANGED METHYLTRANSFERASE 2 (DRM2) protein co-expressed with HISTONE DEACETYLASE 9 (HDA9)-HA in *N. benthamiana* from two biological replicates.

Fig. S4 DOMAINS REARRANGED METHYLTRANSFERASE 2 (DRM2) transgene rescued the loss of DNA methylation in *drm1 drm2* (*dd*) in *Arabidopsis*.

Fig. S5 Immunoblot analysis showing another two biological replicates of Fig. 3(e), the half-life of DOMAINS REARRANGED METHYLTRANSFERASE 2 (DRM2) protein in pDRM2::gDRM2-FLAG/WT and pDRM2::gDRM2-FLAG/*cfk1 Arabidopsis* transgenic seedlings treated with 500 μM cycloheximide (CHX) for the indicated time.

Fig. S6 Characterisation of COP9 SIGNALOSOME INTERACTING F-BOX KELCH 1 (CFK1) OE lines in *Arabidopsis*.

Fig. S7 COP9 SIGNALOSOME INTERACTING F-BOX KELCH 1 (CFK1) regulates CHH DNA methylation in *Arabidopsis*.

Fig. S8 COP9 SIGNALOSOME INTERACTING F-BOX KELCH 1 (CFK1) regulates CHH hypomethylation in *Arabidopsis*.

Fig. S9 DNA methylation is unchanged in *cfk1* mutant at three well studied RdDM targets in *Arabidopsis*.

Table S1 Primer sequences used in this study.

Table S2 List of proteins involved in the ubiquitination pathway from DOMAINS REARRANGED METHYLTRANSFERASE 2 (DRM2) mass spectrometry data.

Table S3 Sequencing depth, coverage and bisulfite conversion rate.

Please note: Wiley Blackwell are not responsible for the content or functionality of any Supporting Information supplied by the authors. Any queries (other than missing material) should be directed to the *New Phytologist* Central Office.